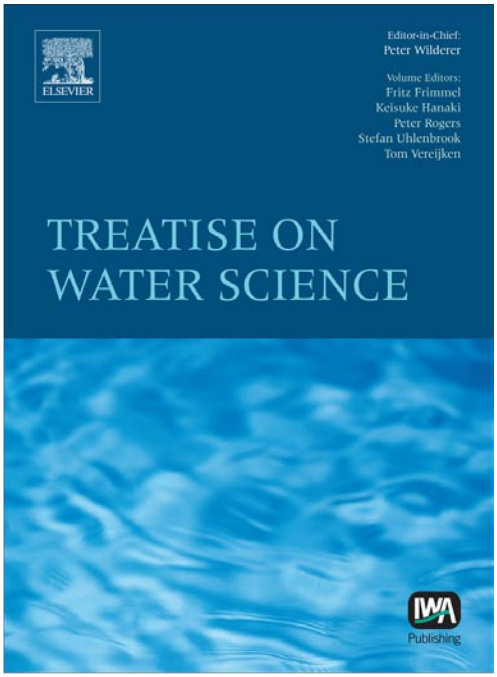

Hopmans JW (2011) Infiltration and Unsaturated Zone. In: Peter Wilderer (ed.) Treatise on Water Science, vol. 2, pp. 103–114 Oxford: Academic Press.

2.05 Infiltration and Unsaturated Zone

JW Hopmans, University of California, Davis, CA, USA

2.05.1	**Introduction**	103
2.05.2	**Soil Properties and Unsaturated Water Flow**	103
2.05.2.1	Soil Water Retention	104
2.05.2.2	Unsaturated Hydraulic Conductivity	105
2.05.2.3	Modeling of Unsaturated Water Flow and Transport	106
2.05.2.4	Infiltration Processes	107
2.05.3	**Infiltration Equations**	109
2.05.3.1	Philip Infiltration Equation	109
2.05.3.2	Parlange *et al.* Model	109
2.05.3.3	Swartzendruber Model	110
2.05.3.4	Empirical Infiltration Equations	110
2.05.4	**Measurements**	110
2.05.4.1	Infiltration	110
2.05.4.2	Unsaturated Water Flow	111
2.05.5	**Scaling and Spatial Variability Considerations**	112
2.05.6	**Summary and Conclusions**	113
Acknowledgments		113
References		113

2.05.1 Introduction

As soils make up the upper part of the unsaturated zone, they are subjected to fluctuations in water and chemical content by infiltration and leaching, water uptake by plant roots, and evaporation from the soil surface. It is the most dynamic region of the subsurface, as changes occur at increasingly smaller time and spatial scales when moving from the groundwater toward the soil surface. Environmental scientists are becoming increasingly aware that soils make up a critically important component of the earth's biosphere, because of their food production and ecological functions, and the soil's important role in controlling water quality. For example, prevention or remediation of soil and groundwater contamination starts with proper management of the unsaturated zone.

Water entry into the soil by infiltration is among the most important soil hydrological processes, as it controls the partitioning between runoff and soil water storage. Runoff water determines surface water quantity and quality, whereas infiltrated water determines plant available water, evapotranspiration, groundwater recharge, and groundwater quality. Also through exfiltration, infiltrated water affects water quality in waterways and associated riparian zones. Despite its relevance and our reliable physical understanding of infiltration, we have generally many difficulties predicting infiltration at any scale. Mostly, this is so because the infiltration rate is a time-varying parameter of which its magnitude is largely controlled by spatially variable soil properties, in both vertical and horizontal directions of a hydrologic basin. Moreover, infiltration rate and runoff are affected by vegetation cover, as it protects the soil surface from the energy impacts of falling raindrops or intercepting rainfall, serving as temporary water storage. The kinetic energy of rainfall causes soil degradation, leading to soil surface sealing and decreasing infiltration.

Historically, solutions to infiltration problems have been presented by way of analytical solutions or empirically. Analytical solutions provide values of infiltration rate or cumulative infiltration as a function of time, making simplifying assumptions of soil depth variations of water content, before and during infiltration. Instead, we now often use powerful computers to conduct numerical simulations of unsaturated water flow to solve for water content and water fluxes throughout the unsaturated soil domain in a single vertical direction or in multiple spatial dimensions, allowing complex initial and boundary conditions. However, although the modeling of multidimensional unsaturated water flow is extremely useful for many vadose zone applications, it does not necessarily improve the soil surface infiltration rate prediction, in light of the large uncertainty of the soil physical properties and initial and boundary conditions that control infiltration. In contrast, empirical infiltration models serve primarily to fit model parameters to measured infiltration, but have limited power as a predictive tool.

2.05.2 Soil Properties and Unsaturated Water Flow

The soil consists of a complex arrangement of mostly connected solid, liquid, and gaseous phases, with the spatial distribution and geometrical arrangement of each phase, and the partitioning of solutes between phases, controlled by physical, chemical, and biological processes. The unsaturated zone is bounded by the soil surface and merges with the groundwater in the capillary fringe. Water in the unsaturated soil matrix is held by capillary and adsorptive forces. Water is a primary factor leading to soil formation from the weathering of parent material such as rock or transported deposits, with additional factors of climate, vegetation, topography, and parent material determining soil physical properties.

Defining the soil's dry bulk density by ρ_b ($M\,L^{-3}$), soil porosity, ε ($L^3\,L^{-3}$), is defined by

$$\varepsilon = 1 - \frac{\rho_b}{\rho_s} \tag{1}$$

with ρ_s being the soil's particle density ($M\,L^{-3}$). Equation (1) shows that soil porosity has lower values as bulk soil density is increased such as by compaction.

Unsaturated water flow is largely controlled by the physical arrangement of soil particles in relation to the water and air phases within the soil's pore space, as determined by pore-size distribution and water-filled porosity or volumetric water content, θ (L^3 water/L^3 bulk soil). The volumetric water content θ expresses the volume of water present per unit bulk soil as

$$\theta = \frac{w\rho_b}{\rho_w} \tag{2}$$

where w is defined as the mass water content (M of water/M dry soil) and we take $\rho_w = 1000\,kg\,m^{-3}$. Alternatively, the soil water content can be described by the degree of saturation S (–) and the equivalent depth of stored water D_e (L), or

$$S = \frac{\theta}{\varepsilon} \quad \text{and} \quad D_e = \theta D_{soil} \tag{3}$$

so that θ can also be defined by the equivalent depth of water per unit depth of bulk soil, D_{soil} (L). The volumetric water content ranges between 0.0 (dry soil) and the saturated water content, θ_s, which is equal to the porosity if the soil were completely saturated. The degree of saturation varies between 0.0 (completely dry) and 1.0 (all pores completely water-filled). When considering water flow, the porosity term is replaced by the saturated water content, θ_s, and both terms in Equation (3) are corrected by subtracting the so-called residual water content, θ_r (soil water content for which water is considered immobile), so that the effective saturation, S_e, is defined as

$$S_e = \frac{\theta - \theta_r}{\theta_s - \theta_r} \tag{4}$$

In addition to the traditional thermogravimetric method to determine soil water content, many other measurement techniques are available, including neutron thermalization, electrical conductivity, dielectric, and heat pulse methods. A recent review on soil moisture measurement methods was presented by Robinson *et al.* (2008), focusing on measurement constraints between the many available methods across spatial scales.

In soils, the driving force for water to flow is the gradient in total water potential. The total potential of bulk soil water can be written as the sum of all possible component potentials, so that the total water potential (ψ_t) is equal to the sum of osmotic, matric, gravitational, and hydrostatic pressure potential. Whereas in physical chemistry the chemical potential of water is usually defined on a molar or mass basis, soil water potential is usually expressed with respect to a unit volume of water, thereby attaining units of pressure (Pa); or per unit weight of water, leading to soil water potential expressed by the equivalent height of a column of water (L). The resulting pressure head equivalent of the combined adsorptive and capillary forces in soils is defined as the matric pressure head, h. When expressed relative to the reference potential of free water, the water potential in unsaturated soils is negative (the soil water potential is less than the water potential of water at atmospheric pressure). Hence, the matric potential decreases or is more negative as the soil water content decreases. In using head units for water potential, the total water potential (H) is defined as the sum of matric potential (h), gravitational potential (z), hydrostatic pressure potential (p), and osmotic potential (π). For most hydrological applications, the contribution of the osmotic potential can be ignored, so that for unsaturated water flow ($p = 0$) the total soil water potential can be written as

$$H = h + z \tag{5}$$

The measurement of the soil water matric potential *in situ* is difficult and is usually done by tensiometers in the range of matric head values larger (less negative) than -6.0 m. A tensiometer consists of a porous cup, usually ceramic, connected to a water-filled tube (Young and Sisson, 2002). The suction forces of the unsaturated soil draw water from the tensiometer into the soil until the water pressure inside the cup (at pressure smaller than atmospheric pressure) is equal to the pressure equivalent of the soil water matric potential just outside the cup. The water pressure in the tensiometer is usually measured by a vacuum gauge or pressure transducer. Other devices that are used to indirectly measure the soil water matric potential include buried porous units (Scanlon *et al.*, 2002), for which either the electrical resistance or the thermal conductivity is measured *in situ*, after coming into hydraulic equilibrium with the surrounding soil (h in sensor and soil are equal). Although widely used, these types of sensors require laboratory calibration, before field installation.

2.05.2.1 Soil Water Retention

The soil water retention function determines the relation between the volume of water retained by the soil, expressed by θ, and the governing soil matric, or suction forces (Dane and Hopmans, 2002). These suction forces are typically expressed by the soil water matric head (strictly negative) or soil suction (strictly positive). These suction forces increase as the size of the water-filled pores decreases, as may occur by drainage, water uptake by plant roots, or soil evaporation. Also known as the soil water release or soil water characteristic function, this soil hydraulic property describes the increase of θ and the size of the water-filled pores with an increase in matric potential, as occurs by infiltration. Since the matric forces are controlled by pore-size distribution, specific surface area, and type of physico-chemical interactions at the solid–liquid interfaces, the soil water retention curve is very soil specific and highly nonlinear. It provides an estimate of the soil's capacity to hold water after irrigation and free drainage (field capacity), minimum soil water content available to the plant (wilting point), and root zone water availability for plants.

The soil water retention curve exhibits hysteresis, that is, the θ value is different for wetting (infiltration) and drying (drainage).

By way of the unique relationship between soil water matric head and the radius of curvature of the air–water interface in the soil pores, and using the analogy between capillary tubes and the irregular pores in porous media, a relationship can be derived between soil water matric head (h) and effective pore radius, r_e, or

$$\rho g h = \frac{2\sigma \cos \alpha}{r_e} \tag{6}$$

where σ and α are defined as the surface tension and wetting angle of wetting fluid with soil particle surface (typically values for σ and α are 0.072 N m^{-1} and 0°, respectively), ρ is the density of water, and g is the acceleration due to gravity (9.8 m s^{-2}). Because of capillary equation, the effective pore-size distribution can be determined from the soil water retention curve in the region where matric forces dominate. Laboratory and field techniques to measure the soil water retention curve, and functional models to fit the measured soil water retention data, such as the van Genuchten (1980) and Brooks and Corey (1964) models, are described by Kosugi *et al.* (2002). Alternatively, knowledge of the particle size distribution may provide information on the shape of the soil water retention curve, as presented by Nasta *et al.* (2009). An example of measured and fitted soil water retention data for two different soils is presented in Figure 1 (Tuli and Hopmans, 2004).

2.05.2.2 Unsaturated Hydraulic Conductivity

The relation between the soil's unsaturated hydraulic conductivity, K, and volumetric water content, θ, is the second essential fundamental soil hydraulic property needed to describe unsaturated soil water flow. K is a function of the water and soil matrix properties, and controls water infiltration and drainage rates, and is strongly affected by water content and possibly by hysteresis. It is defined by the Darcy–Buckingham equation, which relates the soil water flux density to the total driving force for flow, with K being the proportionality factor. Except for special circumstances, the total driving force for water flow in soils is determined by the sum of the matric and gravitational forces, expressed by the total water potential head gradient, $\Delta H/L$ (L L^{-1}), where ΔH denotes the change in total water potential head over the distance L. For vertical flow, the application of Darcy's law yields the magnitude of water flux from

$$q = -K(\theta)\left(\frac{dh}{dz} + 1\right) \tag{7}$$

where q is the Darcy water flux density (L^3 water L^{-2} soil surface T^{-1}) and z defines the vertical position ($z>0$, upwards, L). A soil system is usually defined by the bulk soil, without consideration of the size and geometry of the individual flow channels or pores. Therefore, the hydraulic conductivity (K) describes the ability of the bulk soil to transmit water, and is expressed by volume of water flowing per unit area of bulk soil per unit time (L T^{-1}).

Functional models for unsaturated hydraulic conductivity are based on pore-size distribution, pore geometry, and connectivity, and require integration of soil water retention functions to obtain analytical expressions for the unsaturated hydraulic conductivity. The resulting expressions relate the relative hydraulic conductivity, K_r, defined as the ratio of the unsaturated hydraulic conductivity, K, and the saturated hydraulic conductivity, K_s, to the effective saturation, S_e, and can be written in the following generalized form (Kosugi *et al.*, 2002):

$$K_r(S_e) = S_e^l \left[\frac{\int_0^{S_e} |h|^{-\eta}\, dS_e}{\int_0^{S} |h|^{-\eta}\, dS_e}\right]^{\gamma} \tag{8}$$

where l and η are parameters related to the tortuosity and connectivity of the soil pores, and the value of the parameter γ is determined by the method of evaluating the effective pore radii. For values of $l=0.5$, $\eta=1.0$, and $\gamma=2.0$, Equation (8) reduces to the so-called Mualem (1976) model, that is routinely combined with the van Genuchten (1980) soil water retention model to yield a closed-form expression for the unsaturated hydraulic conductivity function. The moisture dependency is highly nonlinear, with a change in K of five or more orders of magnitude across field-representative changes in unsaturated soil water content. Methods to measure the saturation dependency of the hydraulic conductivity are involved and time consuming. A variety of methods are described in Dane and Topp (2002) and Dirksen (2001). Measurement errors are generally large due to (1) the difficulty of flow measurements in the low water content range and (2) the dominant effect of large pores (macropores), cracks, and fissures in the high water content range. An example of the unsaturated hydraulic conductivity for water, relative to its

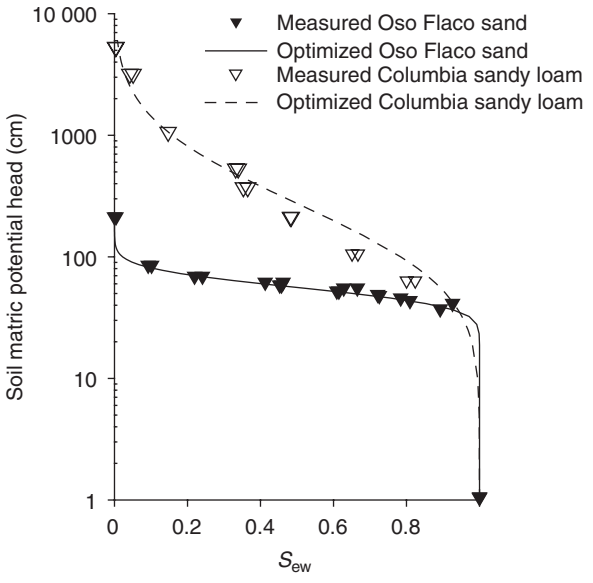

Figure 1 Measured (symbols) and fitted (lines) soil water retention data. From Tuli AM and JW Hopmans (2004) Effect of degree of saturation on transport coefficients in disturbed soils. *European Journal of Soil Science* 55: 147–164.

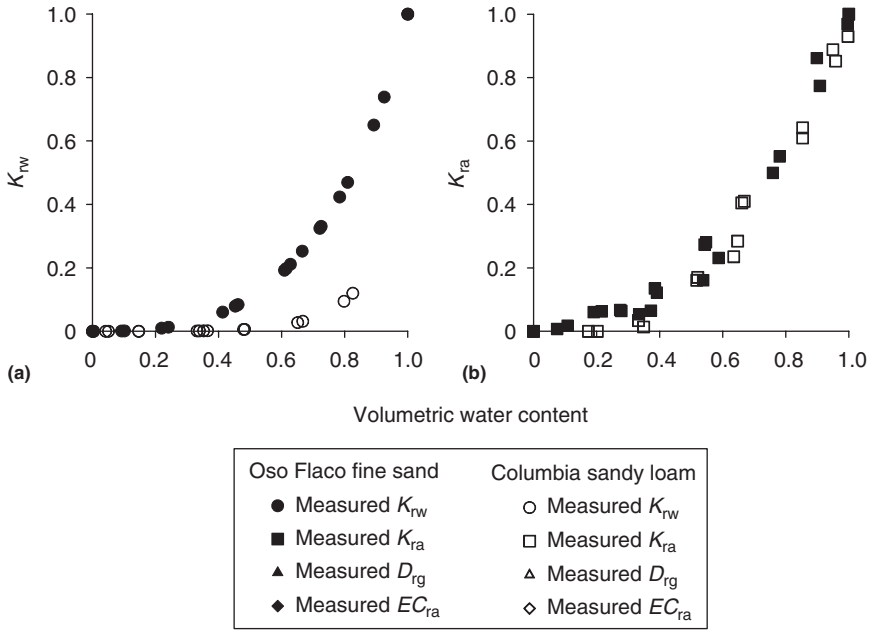

Figure 2 (a) Measured relative hydraulic conductivity for water (K_{rw}) and (b) air conductivity (K_{ra}) as a function of degree of water (S_{ew}) and air (S_{ea}) saturation. From Tuli AM and JW Hopmans (2004) Effect of degree of saturation on transport coefficients in disturbed soils. *European Journal of Soil Science* 55: 147–164.

saturated values (K_{rw}), is presented in Figure 2(a), for the same two soils as in **Figure 1**. We note that θ_s in the vadose zone is typically about 85% of the porosity, so that a saturated soil (e.g., as the result of ponded infiltration) is really a satiated soil due to entrapped air, with a saturated hydraulic conductivity that is significantly smaller than the true K_s.

The unsaturated hydraulic conductivity is related to the intrinsic soil permeability, k (L^2), by

$$K = \frac{\rho g k}{\mu} \tag{9}$$

where μ denotes the dynamic viscosity of water ($F\,T\,L^{-2}$). The usage of permeability instead of conductivity allows application of the flow equation to liquids other than water with different density and viscosity values. In addition to unsaturated hydraulic conductivity, **Figure 2** also includes data for the saturation dependency of the relative air conductivity (K_{ra}), as might be important for water infiltration in soil, when the soil gas phase is trapped and increasing in pressure, so that water infiltration is partly controlled by soil air permeability (Latifi *et al.*, 1994).

2.05.2.3 Modeling of Unsaturated Water Flow and Transport

Numerous studies have been published addressing different issues in the numerical modeling of unsaturated water flow using the Richards' equation. In short, the dynamic water flow equation is a combination of the Darcy expression and a mass balance formulation. Using various solution algorithms, the soil region of interest is discretized in finite-size elements, i, that can be one, two, or three dimensional, to solve for temporal changes in h, θ, or water flux, q, for each element or voxel i at any time t.

Most multidimensional soil water flow models use a finite-element, Picard time-iterative numerical scheme (Šimunek *et al.*, 2008) to solve the Richards equation. For isotropic conditions and one-dimensional vertical flow, the general water flow equation simplifies to

$$\frac{\partial \theta}{\partial t} = \frac{\partial}{\partial z}\left[K(h)\left(\frac{\partial h}{\partial z} + 1\right)\right] - S(z,t) \tag{10}$$

where S ($L^3\,L^{-3}\,T^{-1}$) is the sink term, accounting for root water uptake. Boundary and initial conditions must be included to allow for specified soil water potentials or fluxes at all boundaries of the soil domain. Richards' equation is a highly nonlinear partial differential equation, and is therefore extremely difficult to solve numerically because of the largely nonlinear dependencies of both water content and unsaturated hydraulic conductivity on the soil water matric head. Both the soil water retention and unsaturated hydraulic conductivity relationships must be known *a priori* to solve the unsaturated water flow equation. Specifically, it will need the slope of the soil water retention curve, or water capacity $C(h)$, defined as $C(h) = d\theta/dh$.

As dissolved solutes move through the soils with the water, various physical, chemical, and biological soil properties control their fate. In addition to diffusion and dispersion, fate and transport of chemicals in the subsurface are influenced by sorption to the solid phase and biological transformations. Both diffusion and dispersion of the transported chemical are a function of pore-size distribution and water content. Mechanical or hydrodynamic dispersion is the result of water mixing within and between pores as a result of variations in pore water velocity. Increasing dispersivity values cause greater spreading of the chemical, thereby decreasing peak

concentration. Sorbed chemicals move through the vadose zone slower than noninteracting chemicals, and the degree of sorption will largely depend on mineral type, specific surface area of the solid phase, and organic matter fraction. In addition, biogeochemical processes and radioactive decay affect contaminant concentration, such as by cation exchange, mineral precipitation and dissolution, complexation, oxidation–reduction reactions, and by microbial biodegradation and transformations. However, all these mechanisms depend on soil environmental conditions, such as temperature, pH, water saturation, and redox status, and their soil spatial variations. The solute transport equation is generally referred to as the convection–dispersion equation (CDE), and includes the relevant transport mechanisms to simulate and predict temporal changes in soil solute concentration within the simulation domain (Šimunek *et al.*, 2008).

2.05.2.4 Infiltration Processes

For one-dimensional infiltration, the infiltration rate ($L\,T^{-1}$), $i(t)$, can be defined by Equation (7) at the soil surface (subscript surf), or

$$i(t) = -K(\theta)\left(\frac{\partial h}{\partial z} + 1\right)_{\text{surf}} \tag{11a}$$

Cumulative infiltration $I(t)$, expressed as volume of water per unit soil surface area (L), is defined by

$$I(t) = \int_0^t i(t)\mathrm{d}t \tag{11b}$$

Analytical solutions of infiltration generally assume that the wetted soil profile is homogeneous in texture with uniform initial water content. They also make distinction between ponded ($h > 0$ or p) and nonponded soil surface (unsaturated, $h < 0$) infiltration. The infiltration capacity of the soil is defined by $i_c(t)$, the maximum rate at which a soil can absorb water for ponded soil surface conditions. Its maximal value is at time zero, and decreases with time to its minimum value approaching the soil's saturated hydraulic conductivity, K_s, as the total water potential gradient decreases, and tends to unity, with the downward moving wetting front. As defined by Equation (11b), the soil's cumulative infiltration capacity, $I_c(t)$, is defined by the area under the capacity curve. It represents the maximum amount of water that the soil can absorb at any time. Typically, at the onset of infiltration ($t = 0$), the rainfall rate, $r(t)$, will be lower than $i_c(t)$, so that the infiltration rate is equal to the rainfall rate (i.e., $r(t) < i_c(t)$ for $h_{\text{surf}} < 0$). If at any point in time, the rainfall rate becomes larger than the infiltration capacity, ponding will occur ($h_{\text{surf}} > 0$), resulting in runoff. The time at which ponding occurs is defined as t_p (time to ponding). Thus, the actual infiltration rate will depend on the rainfall rate and its temporal changes. This makes prediction of infiltration and runoff much more difficult for realistic time-variable rainfall patterns.

Therefore, infiltration rate prediction is often described as a function of the cumulative infiltration, I, or $i(I)$, independent of the time domain, and with $i(I)$ curves that are independent of rainfall rate (Skaggs, 1982). An example of such a time-invariant approach is the IDA or infiltrability-depth approximation (Smith *et al.*, 2002). The main IDA assumption is that time periods between small rainfall events are sufficiently small so that soil water redistribution and evaporation between events do not affect infiltration rate. IDA implies that the infiltration rate at any given time depends only on the cumulative infiltration volume, regardless of the previous rainfall history. Following this approach, t_p is defined as the time during a storm event when I becomes equal to $I_c(t_p)$, or

$$R = \int_{t=0}^{t_p} r(t)\mathrm{d}t = I_c(t_p)$$

whereas $i(t) = r(t)$ for $t < t_p$. The time invariance of $i(I)$ holds true also when a layered/sealed soil profile is considered (Mualem and Assouline, 1989).

For illustration purposes, we present a hypothetical storm event with time-varying $r(t)$ in Figure 3 (from Hopmans *et al.*, 2007) in combination with an assumed soil-specific infiltration capacity curve, $i_c(t)$. At what time will ponding occur? It will not be at $t = 7$, when $r(t)$ exceeds i_c for the first time. In order to approximate t_p, we plot both I_c and R for the storm in Figure 4(a), as a function of time and determine t_p as the time at which both curves intersect ($t_p = 13$, for $R = I_c = 110$), since at that time, the cumulative infiltration of the storm is identical to the soil's infiltration capacity. The final corresponding $i(I)$ for this soil and storm event is presented in Figure 4(b), showing that the soil infiltration rate is equal to $r(t)$ until $I = R(t) = I_c(t_p) = 110$, after which the infiltration rate is soil-controlled and determined by $I_c(t)$. More accurate approximations to the time-invariant approach can be found in Sivapalan and Milly (1989) and Brutsaert (2005), using the time compression or time condensation approximation that more accurately estimates infiltration prior to surface ponding.

In addition to whether the soil is ponded or not, solutions of infiltration distinguish between cases with and without gravity effects, as different analytical solutions apply. As Equation (11a) shows, infiltration rate $i(t)$ is determined by both the soil water matric potential gradient, $\mathrm{d}h/\mathrm{d}z$, and gravity. However, at the early stage of infiltration into a relatively dry soil, infiltration rate is dominated by the matric potential gradient so that the gravity effects on infiltration can

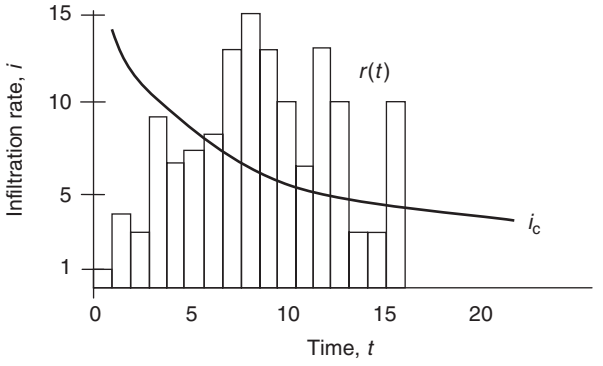

Figure 3 Hypothetical rainfall event, $r(t)$, and soil infiltration capacity, $i_c(t)$. The rainfall event starts at $t = 0$. From Hopmans JW, Assouline S, and Parlange J-Y (2007) Soil infiltration. In: Delleur JW (ed.) *The Handbook of Groundwater Engineering*, pp. 7.1–7.18. Boca Raton, FL: CRC Press.

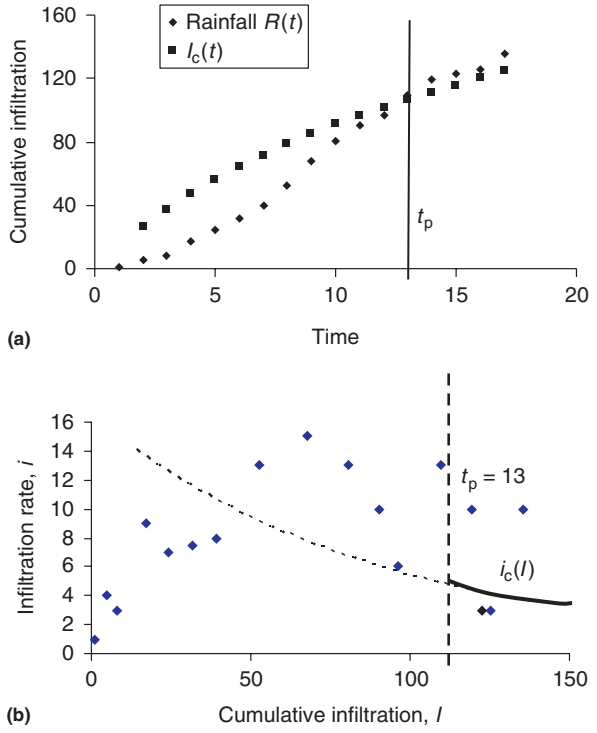

Figure 4 (a) Cumulative infiltration corresponding with infiltration capacity, $I_c(t)$, and cumulative rainfall, $R(t)$ and (b) actual infiltration rate vs. I. Ponding starts only after $t_p = 13$, or $I = 110$. From Hopmans *et al.* (2007).

be ignored. Gravity becomes important in the later stages of infiltration, when the wetting front has moved further down. For gravity-free drainage, a simple analytical solution can be found, after transforming Equation (11a) into a θ-based form by defining the diffusivity $D(\theta) = K(\theta)\mathrm{d}h/\mathrm{d}\theta$, so that

$$i(t) = -D(\theta)\left(\frac{\partial\theta}{\partial z}\right)_{\text{surf}} \tag{12}$$

Using the Boltzmann transformation for a constant head boundary condition (Bruce and Klute, 1956), and defining the scaling variable $\varphi = z/t^{1/2}$, combination of Equations (10) without gravity and sink term and (12) resulted in a unique solution of θ as a function of φ, from which the wetting profile can be computed for any time t (Kirkham and Powers, 1972). Defining θ_1 and θ_0 as the surface water content during infiltration and the initial uniform profile water content, respectively, cumulative infiltration, I, is computed from

$$I = \int_{\theta_0}^{\theta_1} z \; \mathrm{d}\theta = t^{1/2} \int_{\theta_0}^{\theta_1} \varphi \; \mathrm{d}\theta \tag{13a}$$

and results in the simple infiltration equation $I = St^{1/2}$, where the sorptivity S ($\mathrm{L\,T^{-1/2}}$) is defined as

$$S(\theta_1) = \int_{\theta_0}^{\theta_1} \varphi \; \mathrm{d}\theta \tag{13b}$$

Equation (13a) states that for gravity-free infiltration during the early times of vertical infiltration, and at all times for horizontal infiltration, I is a linear function of $t^{1/2}$, with S being defined as the slope of this line. Hence, for saturated soil conditions where $\theta_1 = \theta_s$, the infiltration capacity is computed from $i_c(t) = \frac{1}{2}St^{-1/2}$. Incidentally, this also leads to $I_c = S^2/2i_c$.

A relatively simple analytical solution without and with gravity effects was suggested by Green and Ampt (1911) for a ponded soil surface, with $\theta_{\text{surf}} = \theta_1$. The assumptions are that the wetting front can be approximated as a step function with a constant effective water potential, h_f, at the wetting front, a wetting zone hydraulic conductivity of $K(\theta_1) = K_1 = K_s$, and a constant soil water profile of $\Delta\theta = \theta_1 - \theta_0$. Using this so-called delta-function assumption of a $D(\theta)$ with a Dirac-delta function form, both solutions for horizontal and vertical infiltration can be relatively easily obtained (Jury *et al.*, 1991; Haverkamp *et al.*, 2007). Assuming that K_0 at the initial water content, θ_0, is negligible, the Green and Ampt (GA) solution of vertical infiltration for ponded conditions is ($h = h_{\text{surf}} > 0$):

$$I = I_c = K_1 t + (h_{\text{surf}} - h_f)\Delta\theta \ln\left(1 + \frac{I}{(h_{\text{surf}} - h_f)\Delta\theta}\right) \tag{14}$$

which can be solved iteratively for I. This simple, yet physically based, solution appears to work best for dry coarse-textured soils. A theoretical expression for the wetting front potential head, h_f, was defined by Mein and Farrell (1974), to yield that $h_f = \int_0^{h_0} K_r(h)\mathrm{d}h$, where the relative conductivity $K_r = K(h)/K_s$. The so-called S-form of the GA equation can be obtained by comparing the gravity-free solution of GA with the Boltzmann solution, to yield $S_0^2 = -2K_1 h_f \Delta\theta$:

$$S_1^2(\theta_1) = 2K_1\Delta\theta(h_{\text{surf}} - h_f) = S_0^2 + 2K_1 h_{\text{surf}}\Delta\theta \tag{15a}$$

so that

$$I = K_1 t + h_{\text{surf}}\Delta\theta + \frac{S_0^2}{2K_1}\ln\left(1 + \frac{I}{h_{\text{surf}}\Delta\theta + S_0^2/2K_1}\right) \tag{15b}$$

In reality, the wetting front is not a step function, but will consist of a time-dependent transition zone where water content changes from θ_1 to θ_0. The shape of this transition zone will be a function of time and is controlled by soil type. The step function assumption is better for uniform coarse-textured soils that have a Dirac-like $D(\theta)$, for which there is a sharp decline in K with a decrease in water content near saturation. The wetting front is generally much more diffuse for finer-textured soils that have a wide pore-size distribution.

By now, it must be clear that infiltration and its temporal changes are a function of many different soil factors. In addition to rainfall intensity and duration and the soil physical factors, such as soil water retention and hydraulic conductivity, infiltration is controlled by the initial water content, surface sealing and crusting, soil layering, and the ionic composition of the infiltrated water (Kutilek and Nielsen, 1994; Assouline, 2004). For example, Vandervaere *et al.* (1998) applied the GA model to sealed soil profiles, by assuming that the wetting front potential decreases suddenly as it leaves the seal and enters the soil. This results in a discontinuous drop in the infiltration rate. Many relatively simple infiltration equations have been proposed and are successfully used to

characterize infiltration. This has been achieved despite that these equations apply for homogeneous soils only, in theory.

2.05.3 Infiltration Equations

In addition to the solutions in Section 2.05.2, other physically based analytical solutions have been presented, using different assumptions allowing for a closed-form solution. These can potentially be used to predict infiltration from known soil hydraulic properties of homogeneous soils. However, in practice, this is difficult as soil physical characteristics near the soil surface are time dependent because of soil structural changes and their high spatial variability. Alternatively, various empirical infiltration models have been proposed that are very useful for describing measured infiltration data. A parameter sensitivity analysis of many of the presented infiltration models, analyzing the effects of measurement error, was given by Clausnitzer *et al.* (1998). This section presents the most frequently used infiltration models in both categories.

2.05.3.1 Philip Infiltration Equation

Philip (1957a) presented an analytical infinite-series solution to the water-content-based form of Richards' equation for the case of vertical infiltration:

$$\frac{\partial\theta}{\partial t}=\frac{\partial}{\partial z}\left(D(\theta)\frac{\partial\theta}{\partial z}+K(\theta)\right) \tag{16}$$

For the boundary condition of $h_{surf}=0$ and $\theta_1=\theta_s$, the Philip (1957a) solution converged to the true solution for small and intermediate times, but failed for large times. In this case, an alternative solution was presented (Philip, 1957b). With additional assumptions regarding the physical nature of soil water properties, Philip (1987) proposed joining solutions that are applicable for all times. Philip (1957c) introduced a truncation of the small-time series solution that is a simple two-parameter model equation (PH model):

$$I_c=At+St^{1/2} \tag{17a}$$

which should be accurate for all but very large t, and suitable for applied hydrological studies. The sorptivity S depends on several soil physical properties, including initial water content θ_0, and the hydraulic conductivity and soil water retention functions. S is equal to the expression defined in Equation (13b). Philip (1969) showed that A may take values between $0.38K_s$ and $0.66K_s$. The physical interpretation of A is not straightforward; however, for long times when gravity is dominant and $h_{surf}=0$, one would expect A to be equal to K_s.

Differentiation of Equation (17a) yields the infiltration rate, or

$$i_c=1/2St^{-0.5}+A \tag{17b}$$

Using (17b) to express t as a function of i_c and substituting in Equation (17a) yields $I(i)$, or

$$I=\frac{S^2(i-A/2)}{2(i-A)^2} \tag{17c}$$

For positive pressure heads (h_{surf}), the correction of Equation (15a) to S can be applied. In many cases, values of S and A are obtained from curve fitting. We note that for gravity-free flow, the pH solution without the gravity term corresponds with the Boltzmann solution for horizontal flow in Equation (13).

2.05.3.2 Parlange *et al.* Model

Parlange *et al.* (1982) proposed the following universal model (Parlange *et al.*, model, PA model):

$$t=\frac{S^2}{2K_1^2(1-\delta)}\left[\frac{2K_1}{S^2}I-\ln\frac{\exp\left(\frac{2\delta K_1 I}{S^2}\right)+\delta-1}{\delta}\right] \tag{18a}$$

assuming that K_0 is small so that the ΔK in Parlange *et al.* (1982) is equal to K_1. The value of the parameter δ can be chosen to approach various closed-form solutions. For example, Equation (18a) reduces to the GA solution for δ equal to zero. Its value is a function of $K(\theta)$, and is defined by (Parlange *et al.*, 1985):

$$\delta=\frac{1}{\theta_s-\theta_0}\int_{\theta_0}^{\theta_s}\frac{K_s-K(\theta)}{K_s}d\theta \tag{18b}$$

An approximate value of $\delta=0.85$ was suggested by Parlange *et al.* (1982) for a range of soil types. After taking the time derivative of I, the following $i(I)$-relationship can be derived (Espinoza, 1999):

$$i=K_1+\delta K_1\left(1-\exp\left(\frac{2I\delta K_1}{S^2}\right)\right)^{-1} \tag{18c}$$

Because Equation (18) is based on integration of the water-content-based form of Richards' equation, its theoretical scope is limited to nonponded conditions. A generalization of Equation (18) to include ponded conditions without affecting the value of S was introduced by Parlange *et al.* (1985). Haverkamp *et al.* (1990) presented a modification of their model to include upward water flow by capillary rise. The resulting infiltration model contained six physical parameters, in addition to the interpolation parameter δ (Haverkamp *et al.*, 1990). Both the PA and the Haverkamp *et al.* (1990) model require an iterative procedure to predict $I(t)$. Barry *et al.* (1995) presented an explicit approximation to the Haverkamp *et al.* (1990) model, retaining all six physical parameters (BA model):

$$\begin{aligned}I=&K_1t+\frac{S^2+2K_1h_{surf}\Delta\theta}{2\Delta K}\\&\times\left[t^*+1-\gamma-\exp\left(\frac{-6(2t^*)^{0.5}}{6+(2t^*)^{0.5}}-\frac{2t^*}{3}\right)\right.\\&+\frac{\gamma}{1+t^*}\left\{\exp\left(-\frac{2t^*}{3}\right)[1-(1-\gamma)^8t^{*2.5}]\right.\\&\left.\left.+(2\gamma+t^*)\ln\left(1+\frac{t^*}{\gamma}\right)\right\}\right]\end{aligned} \tag{19a}$$

where

$$t^* = \frac{2t(\Delta K)^2}{S^2 + 2K_1 h_{surf}\Delta\theta}, \quad \gamma = \frac{2K_1(h_{surf} + h_a)\Delta\theta}{S^2 + 2K_1 h_{surf}\Delta\theta} \tag{19b}$$

and h_a denotes the absolute value of the soil water pressure head at which the air phase becomes discontinuous upon wetting. By defining

$$B_1 = (h_{surf} + h_a)\Delta\theta \quad \text{and} \quad B_2 = \frac{2}{S^2 + 2K_1 h_{surf}\Delta\theta} \tag{19c}$$

Equation (19a) can be expressed by only four fitting parameters K_0, K_1, B_1, and B_2. The Clausnitzer *et al.* (1998) study concluded that both the PA and BA models described infiltration equally well; however, the BA model, while most advanced, was not as well suited to serve as a fitting model due to nonuniqueness problems caused by the larger number of fitting parameters.

2.05.3.3 Swartzendruber Model

Swartzendruber (1987) proposed an alternative series solution that is applicable and exact for all infiltration times, and also allows for surface ponding. Its starting point is similar to the GA approach; however, its derivation does not require a step function for the wetted soil profile. Its simplified form is a three-parameter infiltration equation (SW model):

$$I = K_1 t + \frac{S}{A_0}\left(1 - \exp(-A_0 t^{1/2})\right) \tag{20}$$

where A_0 is a fitting parameter of which its value depends on the surface water content, θ_1. As $A_0 \to 0$, it reduces to a form of the Philip (1957b) model with K_1 as the coefficient of the linear term, and for which dI/dt approaches K_1 as $t \to \infty$. As for the GA model, the S-term can be corrected using Equation (15a) to account for ponded conditions.

2.05.3.4 Empirical Infiltration Equations

For most of these types of infiltration equations, the fitting parameters do not have a physical meaning and are evaluated by fitting to experimental data only. However, in many cases, the specific form of the infiltration equation is physically intuitive. For example, the empirical infiltration equation by Horton (1940) is one the most widely used empirical infiltration equations. It considers infiltration as a natural exhaustion process, during which infiltration rate decreases exponentially with time from a finite initial value, $i_c|_{t=0} = (\alpha_1 + \alpha_2)$, to a final value, $\alpha_1 = K_1$. Accordingly, cumulative infiltration I (L) is predicted as a function of time t (HO model):

$$I = \alpha_1 t + \frac{a_2}{a_3}[1 - \exp(-\alpha_3 t)] \tag{21}$$

with the soil parameter $\alpha_3 > 0$, representing the decay of infiltration rate with time. In Equation (21), α_1 can be associated with the hydraulic conductivity (LT^{-1}) of the wetted soil portion, K_1, for $t \to \infty$.

Another simple empirical infiltration equation is the Kostiakov (1932) model (KO):

$$i = at^{-b} \tag{22}$$

Clearly, this equation will not fit infiltration data at long times, as it predicts zero infiltration rate as $t \to \infty$. The value of a should be equal to the infiltration rate at $t = 1$, and $0 < b < 1$.

Mezencev (1948) proposed another infiltration model, and modified the KO model by including a linear term with a coefficient β_1, so that $\beta_1 \to K_1$ for $t \to \infty$ provided $0 < \beta_3 < 1$ and $\beta_2 > 0$ (ME model):

$$I = \beta_1 t + \frac{\beta_2}{1 - \beta_3} t(1 - \beta_3) \tag{23}$$

Other models include the Soil Conservation Service (1972) method and the Holtan solution (Kutilek and Nielsen, 1994; Espinoza, 1999).

2.05.4 Measurements

2.05.4.1 Infiltration

Infiltration measurements can serve various purposes. In addition to characterizing infiltration, for example, to compare infiltration between different soil types, or to quantify macropore flow, it is often measured to estimate the relevant soil hydraulic parameters from the fitting of the infiltration data to a specific physically based infiltration model. This is generally known as inverse modeling. Infiltration is generally measured using one of three different methods: a sprinkler method, a ring infiltration method, or a permeameter method. The sprinkler method is mostly applied to determine time of ponding for different water application rates, whereas the ring infiltrometer method is used when the infiltration capacity is needed. The permeameter method provides a way to measure infiltration across a small range of h-values $\leqslant 0$. A general review of all three methods was recently presented by Smettem and Smith (Smith *et al.*, 2002), whereas a comparison of different infiltration devices using seven criteria was presented by Clothier (2001).

Rainfall sprinklers or rainfall simulators are also sprinkler infiltrometers, but they are typically used to study runoff and soil erosion (e.g., Morin *et al.*, 1967). They mimic the rainfall characteristics (e.g., kinetic energy) of natural storms, specifically the rainfall rate, rainfall droplet size distribution, and drop velocity. Most of these devices measure infiltration by subtracting runoff from applied water. Using a range of water application rates, infiltration measurements can be used to determine the $i(I)$ curve for a specific soil type, with specific soil hydraulic properties such as K_s or S. Various design parameters for many developed rainfall simulators, specifically nozzle systems, were presented by Peterson and Bubenzer (1986). A portable and inexpensive simulator for infiltration measurements along hillslopes was developed by Battany and Grismer (2000). This low-pressure system used a hypodermic syringe needle system to form uniform droplets at rainfall intensities ranging from 20 to 90 mm h^{-1}.

Ring infiltrometers have historically been used to characterize soil infiltration by determining the infiltration capacity, i_c. A ring is carefully inserted in the soil so that water can be ponded over a known area. Since a constant head is required, a constant water level is maintained either by manually adding water and using a measuring stick to maintain a constant depth of ponded water, by using a Mariotte system, or by a valve connected to a float that closes at a predetermined water level. Measurements are usually continued until the infiltration rate is essentially constant. Water seepage around the infiltrometer is prevented by compaction of the soil around and outside of the infiltrometer. Multidimensional water flow under the ring is minimized by pushing the ring deeper into the soil, or by including an outer buffer ring. In the latter case, the soil between the two concentric rings is ponded at the same depth as the inner ring, to minimize lateral flow directed radially outward. The deviation from the assumed one-dimensionality depends on ring insertion depth, ring diameter, measurement time and soil properties such as its hydraulic conductivity, and the presence of restricting soil layers. A sensitivity analysis on diverging flow of infiltrometers was presented by Bouwer (1986) and Wu *et al.* (1997).

Permeameters are generally smaller than infiltrometers and allow easy control of the soil water pressure head at the soil surface. Generally, multidimensionality of flow must be taken into account, using Wooding's (1968) equation for steady flow (Q_∞, $L^3\,T^{-1}$) from a shallow, circular surface pond of free water, or

$$Q_\infty = K_s\left(\pi r_0^2 + \frac{4r_0}{\alpha}\right) \tag{24a}$$

The first and second terms in parentheses denote the gravitational and capillary components of infiltration and α denotes the parameter in Gardner's (1958) unsaturated hydraulic conductivity function:

$$K(h) = K_s \exp(\alpha h) \tag{24b}$$

In this model of the so-called Gardner soil, the macroscopic capillary length, λ_c, is equivalent to $1/\alpha$. The basic analysis for most permeameter methods relies on Wooding's solution. An extensive review of the use of permeameters was presented by Clothier (2001), including the tension infiltrometers and disk permeameters, by which the soil water pressure at water entry is controlled by a bubble tower. Their use is relatively simple, and based on analytical solutions of steady-state water flow. The permeameter method is economical in water use and portable. The soil hydraulic properties (S and K), in an inverse way, can be inferred from measurements using (1) both short- and long-time observations, (2) disks with various radii, or (3) using multiple water pressure heads. Transient solutions of infiltration may be preferable, as it allows analysis of shorter infiltration times, so that the method is faster and likely will better satisfy the homogeneous soil assumption. Differences between one- and three-dimensional solutions for transient infiltration were analyzed by Haverkamp *et al.* (1994), Vandervaere *et al.* (2000), and Smith *et al.* (2002) from multidimensional numerical modeling analysis. These effects were reported to be small if gravity effects were included. Nowadays, permeameters are most often applied to estimate the soil's hydraulic characteristics in an inverse way, by fitting infiltration data to analytical solutions. In many cases, auxiliary water content or matric potential data are required to yield unique solutions.

2.05.4.2 Unsaturated Water Flow

Whereas infiltration measures are typically conducted along the soil surface only, measurement of unsaturated water flow requires installation of instruments and sensors below ground, thereby largely complicating measurement procedures and analysis. The simplest expression for unsaturated water flow estimation is the Darcy equation (7), but still requires the measurement of soil water content (θ) or soil water matric potential (h) at various soil depths, and knowledge of the unsaturated hydraulic function, $K(\theta)$, as expressed by Equation (8). Installation of soil moisture or potential sensors requires extreme care, because of issues of soil disturbance, inadequate soil sensor contact, and inherent soil heterogeneities. In addition, it is not always straightforward to determine installation depth of sensors, as it will depend on *a priori* knowledge of soil horizon differentiation. Inherently problematic is the fact that no soil water flux meters are available to accurately measure the unsaturated soil water flux q in Equation (7). A review by Gee *et al.* (2003) provides possible direct and indirect methods, but none of them are adequate because of problems with divergence of water flow near the flux measurement device. Recently, the heat pulse probe was developed (Kamai *et al.*, 2008) for indirect measurement of soil water flux, but is limited to fluxes of 6 mm d^{-1} or higher. Finally, very few routine measurements are available to determine the $K(\theta)$ relationship. In fact, the lack of the unsaturated conductivity information is the most limiting factor of *in situ* application of the Darcy equation. Most promising is the application of inverse modeling for parameter estimation of the soil hydraulic functions, using both laboratory and field techniques (Hopmans *et al.*, 2002b), which can be used in conjunction with *in situ* water content and soil water potential measurements to estimate temporal changes in depth distribution of soil water flux.

Selected steady-state solutions are provided in Jury *et al.* (1991), but are only of limited use for real field conditions since soil water content and matric potential values change continuously. Most realistically, one must apply the transient unsaturated water flow (Equation (10)) that arises from combination of the Darcy equation with mass conservation. However, its solution also requires *a priori* knowledge of the soil water capacity, C, as determined from the slope of the soil water retention curve, and time measurements of θ and h, at the various soil horizon interfaces and at the boundaries of the soil domain of interest, including at the soil profile bottom. Although certainly possible, relatively few of such field experiments are conducted routinely because they are time consuming and wrought with complications. However, in combination with inverse modeling, such field experiments can provide a wealth of information, including plant root water uptake dynamics, plant transpiration, and drainage rates (Vrugt *et al.*, 2001). Therefore, large lysimeters with selected

water content and soil water potential measurements may be very useful.

2.05.5 Scaling and Spatial Variability Considerations

Soil hydrologists need to apply locally measured soil physical data to characterize flow and transport processes at large-scale heterogeneous vadose zones. For example, prediction of soil water dynamics, such as infiltration at the field scale, is usually derived from the measurement of soil hydraulic properties from laboratory cores, as collected from a limited number of sampling sites across large spatial extents. Soil parameters obtained from these small-scale measurements are subsequently included in numerical models with a grid or element size many times larger, with the numerical results extrapolated to predict large-scale flow and transport behavior. Because of the typical nonlinearity of soil physical properties, their use across spatial scales is inherently problematic. Specifically, the averaging of processes determined from discrete small-scale samples may not describe the true soil behavior involving larger spatial structures. Moreover, the dominant physical flow processes may vary between spatial scales. Considering that soil physical, chemical, and biological measurements are typically conducted for small measurement volumes and that the natural variability of soils is enormous, the main question asked is how small-scale measurements can provide information about large-scale flow and transport behavior. In their treatise of scale issues of vadose zone modeling, Hopmans *et al.* (2002a) offer a conceptual solution, considering the control of small-scale processes on larger-scale flow behavior. Hence, vadose zone properties are nonunique and scale dependent, resulting in effective properties that vary across spatial scales and merely serve as calibration parameters in simulation models. Therefore, their accurate prediction in heterogeneous materials can only be accomplished using scale-appropriate measurements, including those that measure at the landscape scale.

In addition, infiltration measurements are typically conducted at measurement scales in the range of 0.2–1.0 m. This is relevant for irrigation purposes, especially for micro-irrigation applications. Yet, infiltration information is often needed for much larger spatial scales, at the pedon scale, hillslope scale, and watershed scale. Very little work has been done relating infiltration process to measurement or support scale. Exceptions are the studies by Sisson and Wierenga (1981) and Haws *et al.* (2004), who measured steady-state infiltration at three spatial scales, ranging from 5 to 127-cm-diameter infiltrometer rings. Their results showed that much of the larger-scale infiltration occurs through smaller-scale regions, and that the spatial variability of infiltration decreased as the measurement scale increased. Thus, in general, we find that the process of infiltration might vary with spatial scale, and that larger spatial scales are required to estimate representative infiltration characteristics across a typical landscape.

Many field studies have dealt with the significant areal heterogeneity of soil hydraulic properties, and particularly that of the saturated hydraulic conductivity, K_s (Nielsen *et al.*, 1973). The heterogeneity in K_s is recognized to have a major effect on unsaturated flow, leading to significant variation in local infiltration. In general, accounting for areal heterogeneity leads to shorter ponding times and to a more gradual decrease of the infiltration flux with time (Smith and Hebbert, 1979; Sivapalan and Wood, 1986). To characterize spatial variable infiltration rates, Sharma *et al.* (1980) measured infiltration with a double-ring infiltrometer at 26 sites in a 9.6-ha watershed. The infiltration data were fitted to the PH infiltration Equation (17a), and fitting parameters S and A were scaled to express their spatial variability and to describe the ensemble-average or composite infiltration curve of the watershed. A simpler but similar scaling technique for infiltration data was presented by Hopmans (1989), who measured transient infiltration at 50 sites along a 100-m transect. Data were fitted to both the PH and a modified KO model that includes an additional constant c as a second term in Equation (23). This paper showed that spatial variability of infiltration can be easily described by the probability density function of a single scaling parameter, to be used for applications in Monte Carlo simulation of watershed hydrology, as suggested for the first time by Peck *et al.* (1977). For application at the field scale, the so-called one-point method was presented by Shepard *et al.* (1993) to estimate furrow-average infiltration parameters of PH Equation (17a), across a furrow-irrigated agricultural field. They used the volume-balance principle from furrow advance time across the field, water inflow rate, and flow area measurements.

For modeling surface hydrology, by subtracting the infiltration rate, $i(t)$, from the rainfall rate, $r(t)$, it is possible to estimate spatial and temporal distributions of rainfall excess or runoff. The influence of spatial heterogeneity in rainfall and soil variability on runoff production was studied by Sivapalan and Wood (1986) from an analytical solution of infiltration and making use of the IDA approximation. Statistical characteristics of ponding time and infiltration rate were presented for two cases, one with a spatially variable soil with a log-normal K_s distribution and uniform rainfall, and the other for a homogeneous soil with spatially variable rainfall. Among the various results, this study concluded that the ensemble infiltration approach is biased for spatially variable soils. Their results also showed that the cumulative distribution of ponding times or proportion of ponded area is an excellent way of analyzing mean areal infiltration. Moreover, the spatial correction of infiltration rate is time dependent and varies depending on the correlation lengths of rainfall and soil K_s. This study neglected the effects of surface water run-on, as caused by accumulated water upstream, running on to neighboring areas, thereby contributing locally to infiltration. A quantitative analysis of soil variability effects on watershed hydraulic response that included surface water interactions, such as run-on, was presented by Smith and Hebbert (1979), through analysis of the effects of deterministic changes of infiltration properties in the direction of surface water flow, using a kinematic watershed model. In a subsequent study by Woolhiser *et al.* (1996), it was clearly demonstrated that runoff hydrographs along a hillslope are significantly affected by spatial trends in the soil's saturated hydraulic conductivity. We expect that important new information can be collected by linking this interactive modeling approach with remote sensing and geographical information system (GIS) tools. A detailed analysis and review of the control of spatially

variable hydrologic properties on overland flow are presented by Govindaraju *et al.* (2007).

Yet another concern regarding nonideal infiltration, causing spatially variable infiltration at small spatial scales, comes from the presence of water-repellent or hydrophobic soils. Since the 1980s much new research and findings have been presented, improving the understanding of the underlying physical processes and its relevance to soil water flow and water infiltration (DeBano, 2000; Wang *et al.*, 2000). Infiltration may be controlled by soil surface crust-forming dynamics, which is another complex phenomenon dominated by a wide variety of factors involving soil properties, rainfall characteristics, and local water flow conditions. Two types of rainfall-induced soil seals can be identified: (1) structural seals that are directly related to rainfall through the impact of raindrops and sudden wetting and (2) depositional or sedimentary seals that are indirectly related to rainfall as it results from the settling of fine particles carried in suspension by runoff in soil depressions. A recent review on concepts and modeling of rainfall-induced soil surface sealing was presented by Assouline (2004).

2.05.6 Summary and Conclusions

Although important and seemingly simple, infiltration is a complicated process that is a function of many different soil properties, rainfall, land use, and vegetation characteristics. In addition to rainfall intensity and duration as well as the soil physical factors, such as soil water retention and hydraulic conductivity, infiltration is controlled by the initial water content, surface sealing and crusting, hydrophobicity, soil layering, and the ionic composition of the infiltrated water. Many relatively simple infiltration equations have been proposed historically, and are successfully used to characterize infiltration. Other physically based analytical solutions have been presented that can potentially be used to predict infiltration. However, in practice, this is difficult as soil physical characteristics near the soil surface show naturally high soil spatial variability and are often time dependent because of soil structural changes. Alternatively, infiltration is often measured to estimate the relevant soil hydraulic parameters from the fitting of the infiltration data to a specific infiltration model by inverse modeling, such as by using permeameters.

Whereas most infiltration measurement techniques and infiltration models apply to relatively small spatial scales, infiltration information is often needed at the watershed and hillslope scales. Yet, it has been shown that much of the larger-scale infiltration occurs through smaller-scale regions, for example, because infiltration is largely controlled by spatial variations of the soil's physical characteristics at the land surface, vegetation cover, and topography. In general, we expect that the process of infiltration varies with spatial scale, and that measurements at larger spatial scales are needed to estimate representative infiltration characteristics across hillslope and larger spatial scales. For that purpose, improved solutions to infiltration across scales from the field to basin scale are needed, such as may become available using rapidly developing techniques including remote sensing, GIS, and new measurement devices.

Acknowledgments

This chapter is partly based on the paper by Hopmans *et al.* (2007), and includes edited sections of that paper. The author acknowledges the significant input received by Drs. J.-Y Parlange and S. Assouline in writing the 2007 paper.

References

Assouline S (2004) Rainfall-induced soil surface sealing: A critical review of observations, conceptual models and solutions. *Vadose Zone Journal* 3: 570–591.

Barry DA, Parlange J-Y, Haverkamp R, and Ross PJ (1995) Infiltration under ponded conditions: 4. An explicit predictive infiltration formula. *Soil Science* 160: 8–17.

Battany MC and Grismer ME (2000) Development of a portable field rainfall simulator for use in hillside vineyard runoff and erosion studies. *Hydrological Processes* 14: 1119–1129.

Bouwer H (1986). Intake rate: Cylinder infiltrometer, In: Klute A, (ed.) *Methods of Soil Analysis, Part 1.* Number 9 in the Series Agronomy, pp. 825–844. Madison, WI: American Society of Agronomy.

Brooks RH and Corey AT (1964) *Hydraulic Properties of Porous Media*, Hydrology Paper No. 3. Fort Collins, CO: Colorado State University.

Bruce RR and Klute A (1956) The measurement of soil moisture diffusivity. *Soil Science Society American Proceedings* 20: 458–462.

Brutsaert W (2005) *Hydrology – An Introduction.* New York, NY: Cambridge University Press.

Clausnitzer V, Hopmans JW, and Starr JL (1998) Parameter uncertainty analysis of common infiltration models. *Soil Science Society of America Journal* 62: 1477–1487.

Clothier BE (2001) Infiltration. In: Smith KA and Mullins CE (eds.) *Soil and Environmental Analysis, Physical Methods*, 2nd edn., Revised and Expanded, pp. 239–280. New York: Dekker.

Dane JH and Hopmans JW (2002) Soil water retention and storage – introduction. In: Dane JH and Topp GC (eds.) *Methods of Soil Analysis. Part 4. Physical Methods*, pp. 671–674. Madison, WI: Soil Science Society of America.

Dane JH and Topp GC (eds.) (2002) *Methods of Soil Analysis. Part 4. Physical Methods*, vol. 5, Madison, WI: Soil Science Society of America.

DeBano LF (2000) Water repellency in soils: A historical overview. *Journal of Hydrology* 231: 4–32.

Dirksen C (2001) Hydraulic conductivity. In: Smith KA and Mullins CE (eds.) *Soil and Environmental Analysis*, pp. 141–238. New York: Dekker.

Espinoza RD (1999) Infiltration. In: Delleur JW (ed.) *The Handbook of Groundwater Engineering*, pp. 7.1–7.18. Boca Raton, FL: CRC Press.

Gardner WR (1958) Some steady state solutions of unsaturated moisture flow equations with application to evaporation from a water table. *Soil Science* 85: 228–232.

Gee GW, Zhang F, and Ward AL (2003) A modified vadose zone fluxmeter with solution collection capability. *Vadose Zone Journal* 2: 627–632.

Govindaraju RS, Nahar N, Corradini C, and Morbidelli R (2007) Infiltration and run-on under spatially-variable hydrologic properties. In: Delleur JW (ed.) *The Handbook of Groundwater Engineering*, pp. 8.1–8.15. Boca Raton, FL: CRC Press.

Green WA and Ampt GA (1911) Studies on soils physics: 1. The flow of air and water through soils. *Journal of Agricultural Science* 4: 1–24.

Haverkamp R, Debionne S, Viallet P, Angulo-Jaramillo R, and de Condappa D (2007) Soil properties and moisture movement in the unsaturated zone. In: Delleur JW (ed.) *The Handbook of Groundwater Engineering*, pp. 6.1–6.59. Boca Raton, FL: CRC Press.

Haverkamp R, Parlange J-Y, Starr JL, Schmitz G, and Fuentes C (1990) Infiltration under ponded conditions: 3. A predictive equation based on physical parameters. *Soil Science* 149: 292–300.

Haverkamp R, Ross PJ, Smettem KRJ, and Parlange J-Y (1994) Three-dimensional analysis of infiltration from the disc infiltrometer. 2. Physically based infiltration equation. *Water Resources Research* 30: 2931–2935.

Haws NW, Boast CW, Rao PSC, Kladivko EJ, and Franzmeier DP (2004) Spatial variability and measurement scale of infiltration rate on an agricultural landscape. *Soil Science Society of America Journal* 68: 1818–1826.

Hopmans JW (1989) Stochastic description of field-measured infiltration data. *Transactions of the American Society of Agricultural Engineers* 32: 1987–1993.

Hopmans JW, Assouline S, and Parlange J-Y (2007) Soil infiltration. In: Delleur JW (ed.) *The Handbook of Groundwater Engineering*, pp. 7.1–7.18. Boca Raton, FL: CRC Press.

Hopmans JW, Nielsen DR, and Bristow KL (2002a) How useful are small-scale soil hydraulic property measurements for large-scale vadose zone modeling. In: Smiles D, Raats PAC, and Warrick A (eds.) *Heat and Mass Transfer in the Natural Environment, the Philip Volume*. Geophysical Monograph Series No. 129, pp. 247–258. Washington, DC: American Geophysical Union.

Hopmans JW, Šimunek J, Romano N, and Durner W (2002b) Inverse methods. In: Dane JH and Topp GC (eds.) *Methods of Soil Analysis. Part 4. Physical Methods*, pp. 963–1008. Madison, WI: Soil Science Society of America.

Horton RE (1940) An approach towards a physical interpretation of infiltration capacity. *Soil Science Society American Proceedings* 5: 399–417.

Jury WA, Gardner WR, and Gardner WH (1991) *Soil Physics*. New York: Wiley.

Kamai T, Tuli A, Kluitenberg GJ, and Hopmans JW (2008) Soil water flux density measurements near 1 cm/day using an improved heat pulse probe. *Water Resources Research* 44: doi: 10.1029/2008WR007036.

Kirkham D and Powers WL (1972) *Advanced Soil Physics*. New York: Wiley.

Kostiakov AN (1932) On the dynamics of the coefficient of water percolation in soils and on the necessity of studying it from a dynamic point of view for purposes of amelioration. In: *Transactions of the Sixth Commission of the International Society of Soil Science A*, pp. 17–21.

Kosugi K, Hopmans JW, and Dane JH (2002) Water retention and storage – parametric models. In: Dane JH and Topp GC (eds.) *Methods of Soil Analysis. Part 4. Physical Methods*, pp. 739–758. Madison, WI: Soil Science Society of America.

Kutilek M and Nielsen DR (1994) *Soil Hydrology. GeoEcology Textbook*. Cremlingen-Destedt. Germany: Catena Verlag.

Latifi H, Prasad SN, and Helweg OJ (1994) Air entrapment and water infiltration in two-layered soil column. *Journal of Irrigation and Drainage Engineering* 120: 871–891.

Mein RG and Farrell DA (1974) Determination of wetting front suction in the Green–Ampt equation. *Soil Science Society of America Proceedings* 38: 872–876.

Mezencev VJ (1948) Theory of formation of the surface runoff (Russian). *Meteorologia i Gidrologia* 3: 33–40.

Morin J, Goldberg D, and Seginer I (1967) A rainfall simulator with a rotating disc. *Transactions of the American Society of Agricultural Engineers* 10: 74–77.

Mualem Y (1976) A new model for predicting the hydraulic conductivity of unsaturated porous media. *Water Resources Research* 12: 513–522.

Mualem Y and Assouline S (1989) Modeling soil seal as a non-uniform Layer. *Water Resources Research* 25: 2101–2108.

Nasta P, Kamai T, Chirico GB, Hopmans JW, and Romano N (2009) Scaling soil water retention functions using particle-size distribution. *Journal of Hydrology* 374: 223–234.

Nielsen DR, Biggar JB, and Ehr KT (1973) Spatial variability of field measured soil water properties. *Hilgardia* 42: 215–260.

Parlange J-Y, Haverkamp R, and Touma J (1985) Infiltration under ponded conditions: 1. Optimal analytical solution and comparison with experimental observations. *Soil Science* 139: 305–311.

Parlange J-Y, Lisle I, Braddock RD, and Smith RE (1982) The three-parameter infiltration equation. *Soil Science* 133: 337–341.

Peck AJ, Luxmoore RJ, and Stolzy JL (1977) Effects of spatial variability of soil hydraulic properties in water budget modeling. *Water Resources Research* 13: 348–354.

Peterson AE and Bubenzer GD (1986). Intake rate: Sprinkler infiltrometer, In: Klute A, (ed.) *Methods of Soil Analysis, Part 1*. Number 9 in the series Agronomy, pp. 45–870. Madison, WI: American Society of Agronomy.

Philip JR (1957a) The theory of infiltration: 1. The infiltration equation and its solution. *Soil Science* 83: 345–357.

Philip JR (1957b) The theory of infiltration: 2. The profile at infinity. *Soil Science* 83: 435–448.

Philip JR (1957c) The theory of infiltration: 4. Sorptivity and algebraic infiltration equations. *Soil Science* 84: 257–264.

Philip JR (1969) Theory of infiltration. In: Chow VT (ed.) *Advances in Hydroscience*, vol. 5, pp. 215–296. New York, NY: Academic Press.

Philip JR (1987) The infiltration joining problem. *Water Resources Research* 12: 2239–2245.

Robinson DA, Campbell CS, Hopmans JW, *et al*. (2008) Soil moisture measurement for ecological and hydrological watershed-scale observatories: A review. *Vadose Zone Journal* 7: 358–389.

Scanlon BR, Andraski BJ, and Bilskie J (2002) Miscellaneous methods for measuring matric or water potential. In: Dane JH and Topp GC (eds.) *Methods of Soil Analysis. Part 4. Physical Methods*, pp. 643–670. Madison, WI: Soil Science Society of America.

Sharma ML, Gander GA, and Hunt CG (1980) Spatial variability of infiltration in a watershed. *Journal of Hydrology* 45: 101–122.

Shepard JS, Wallender WW, and Hopmans JW (1993) One-point method for estimating furrow infiltration. *Transactions of American Society of Agricultural Engineers* 36: 395–404.

Šimunek J, Van Genuchten MTh, and Sejna M (2008) Development and applications of the HYDRUS and STANMOD software packages and related codes. *Vadose Zone Journal* 7: 587–600.

Sisson JB and Wierenga PJ (1981) Spatial variability of steady-state infiltration rates as a stochastic process. *Soil Science Society of America Journal* 45: 699–704.

Sivapalan M and Milly PCD (1989) On the relationship between the time condensation approximation and the flux-concentration relation. *Journal of Hydrology* 105: 357–367.

Sivapalan M and Wood EF (1986) Spatial heterogeneity and scale in the infiltration response of catchments. In: Gupta VK, Rodriguez-Iturbe I, and Wood EF (eds.) *Scale Problems in Hydrology*, pp. 81–106. Hingham, MA: Reidel.

Skaggs RW (1982) Infiltration, In: Haan CT, Johnson HP, and Brakensiek DL, (eds.) *Hydrologic Modeling of Small Watersheds*, ASAE Monograph No. 5, 121–166. St. Joseph, MI: ASAE.

Smith RE and Hebbert RHB (1979) A Monte-Carlo analysis of the hydrologic effects of spatial variability of infiltration. *Water Resources Research* 15: 419–429.

Smith RE, Smettem KRJ, Broadbridge P, and Woolhiser DA (2002) *Infiltration Theory for Hydrologic Applications*. Water Resources Monograph 15, Washington, DC: American Geophysical Union.

Soil Conservation Service (1972) Estimation of direct runoff from storm rainfall *National Engineering Handbook, Section 4: Hydrology*, pp. 10.1–10.24. Washington, DC: USDA.

Swartzendruber D (1987) A quasi-solution of Richards' equation for the downward infiltration of water into soil. *Water Resources Research* 23: 809–817.

Tuli AM and Hopmans JW (2004) Effect of degree of saturation on transport coefficients in disturbed soils. *European Journal of Soil Science* 55: 147–164.

Vandervaere J-P, Vauclin M, and Elrick DE (2000) Transient flow from tension infiltrometers: I. The two-parameter equation. *Soil Science Society of America Journal* 64: 1263–1272.

Vandervaere J-P, Vauclin M, Haverkamp R, Peugeot C, Thony J-L, and Gilfedder M (1998) Prediction of crust-induced surface runoff with disc infiltrometer data. *Soil Science* 163: 9–21.

Van Genuchten MTh (1980) A closed-form equation for predicting the hydraulic conductivity of unsaturated soils. *Soil Science Society of America Journal* 44: 892–898.

Vrugt JA, Hopmans JW, and Šimunek J (2001) Calibration of a two-dimensional root water uptake model. *Soil Science Society of America Journal* 65: 1027–1037.

Wang Z, Wu QJ, Wu L, Ritsema CJ, Dekker LW, and Feyen J (2000) Effects of soil water repellency on infiltration rate and flow instability. *Journal of Hydrology* 231: 265–276.

Wooding RA (1968) Steady infiltration from a shallow circular pond. *Water Resources Research* 4: 1259–1273.

Woolhiser DA, Smith RE, and Giraldez J-V (1996) Effects of spatial variability of saturated hydraulic conductivity on Hortonian overland flow. *Water Resources Research* 32: 671–678.

Wu L, Pan L, Robertson MJ, and Shouse PJ (1997) Numerical evaluation of ring-infiltrometers under various soil conditions. *Soil Science* 162: 771–777.

Young MH and Sisson JB (2002) Tensiometry. In: Dane JH and Topp GC (eds.) *Methods of Soil Analysis, Part 4: Physical Methods*, pp. 575–606. Madison, WI: Soil Science Society of America.

Relevant Websites

http://www.decagon.com
Decagon Devices, Mini-Disk Infiltrometer.

http://hopmans.lawr.ucdavis.edu
Jan W. Hopmans, Vadose Zone Hydrology.

http://www.pc-progress.com
PC-Progress: Engineering Software Developer; HYDRUS 2D/3 D for Windows, Version 1.xx.

http://ag.arizona.edu/sssa-s1
SSSA Soil Physics Division S-1.

http://en.wikipedia.org
Wikipedia, Infiltration (Hydrology).